

## First determination of dissolution rates of oriented $\text{UO}_2$ single crystals.

S. BERTOLOTTO<sup>1,2</sup>, S. SZENKNECT<sup>2</sup>, S. LALLEMAN<sup>1</sup>, R. PODOR<sup>2</sup>, L. CLAPAREDE<sup>2</sup>, A. MAGNALDO<sup>1</sup>, P. RAISON<sup>3</sup>, B. ARAB-CHAPELET<sup>1</sup> and N. DACHEUX<sup>2</sup>.

<sup>1</sup> CEA, DEN, DMRC, Univ Montpellier, Marcoule, France

<sup>2</sup> ICSM, CEA, CNRS, ENSCM, Univ Montpellier, Site de Marcoule, BP 17171, 30207 Bagnols-Sur-Cèze cedex, France

<sup>3</sup> JRC Karlsruhe, 76344 Eggenstein-Leopoldshafen, Germany

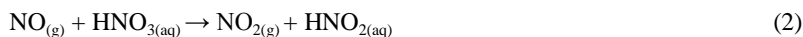
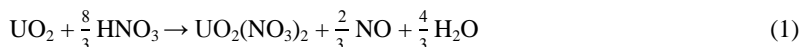
### Abstract Text:

*Millimetre oriented  $\text{UO}_2$  single crystals were cut and oriented at JRC Karlsruhe, with the Laue diffraction. Single crystals have a form of a slab which each side is oriented, therefore one sample owns several surface orientations ((111), (100), (110)...). The area ratios for all oriented surfaces were determined. Then structural characterization was performed on the main surface in order to confirm the surface orientation after their mechanical polishing. The dissolution of the three samples in nitric acid media was realised under dynamic conditions, at room temperature. During dissolution, two steps were observed for all samples. The first step is the same for all samples, so during this step the oriented surface has no impact on dissolution. However concerning the second step, surface's orientation influenced the normalised dissolution rate. The (110) surface was found to dissolve faster than the (100) surface. One explanation could involve the atomic composition of the plans of which each oriented surface is made.*

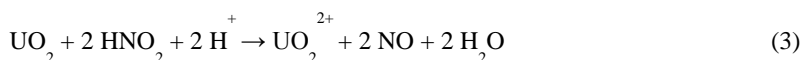
### INTRODUCTION

After its stay for several years in a nuclear reactor, French spent nuclear fuel (SNF) is reprocessed in order to recover the uranium and plutonium it still contained. The head-end step of the processes is the dissolution of  $\text{UO}_2$  in concentrated and hot

nitric acid. SNF is heterogeneous in terms of microstructure, elementary composition and distribution which could significantly influence the dissolution rates. At the present time, dissolution mechanisms are usually described using a simplified solid/liquid interface, and a succession of two steps. The first one was defined by Hermann *et al*<sup>1</sup>, according to equation (1):



While the second one can be described as:



The first step is associated to a slow rate of reaction but forms powerful oxidising species like dissolved NO<sub>x</sub> gases or nitrous acid which is suspected to react again on the surface of UO<sub>2</sub> and induce a catalytic effect on the dissolution<sup>2</sup>.

Dissolution rate is also influenced by the evolution of the solid surface during the dissolution caused by the heterogeneous attack of the solid<sup>3,4</sup>. In order to estimate the impact of the microstructure of the solid on the dissolution rate, samples free from any microstructure like grains boundaries and pores have to be considered. For this reason, single crystals of UO<sub>2</sub> were used. Samples have a slab form and so they have different oriented surfaces, this fact allows access to dissolution rates of UO<sub>2</sub> for several crystallographic orientations.

## EXPERIMENT

### Materials

Millimetre-sized single crystals of UO<sub>2</sub> were prepared from a bigger single crystal produced by melting and very slow cooling of a depleted UO<sub>2</sub> solution in South Africa a long time ago. The samples were cut then oriented at the JRC Karlsruhe thanks to the Laue diffraction method. In this study, three slabs with orientated faces were considered (fig. 1). These orientations were investigated because they were characteristic of the fluorite-type structure.

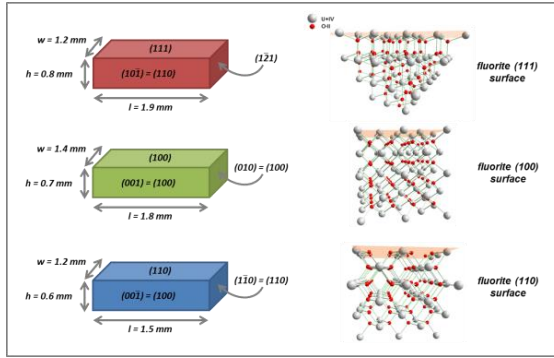


Figure 1. Description of  $\text{UO}_2$  samples in terms of size, faces orientations and surfaces crystallographic structures.

The first step of the samples characterization was to control their weight and dimensions with an optical microscope in order to determine the area ratios for all oriented surfaces (Table 1). During dissolution tests samples were pasted on a support, therefore total surface area in nitric acid media and then the oriented surface ratios are slightly different.

Table 1. Characteristics of  $\text{UO}_2$  single crystals in terms of global surface area and relative surface areas for each orientation (bulk material and during dissolution experiments).

Sample	m (t = 0) (g) $\pm 0.0001$	Total surface area ( $\text{m}^2$ )	(100) oriented surface area (%)	(110) oriented surface area (%)	(111) oriented surface area (%)	( $\bar{1}\bar{2}\bar{1}$ ) oriented surface area (%)
R	0.0233	$9.9 \times 10^{-6}$	/	20	49	31
G	0.0196	$9.7 \times 10^{-6}$	100	/	/	/
B	0.0118	$6.9 \times 10^{-6}$	21	79	/	/
Sample		Total surface area in nitric media $S_T$ ( $\text{m}^2$ )	(100) oriented surface area in nitric media $S_{(100)}$ (%)	(110) oriented surface area in nitric media $S_{(110)}$ (%)	(111) oriented surface area in nitric media $S_{(111)}$ (%)	( $\bar{1}\bar{2}\bar{1}$ ) oriented surface area in nitric media $S_{(\bar{1}\bar{2}\bar{1})}$ (%)
R		$7.5 \times 10^{-6}$	/	27	32	41
G		$7.1 \times 10^{-6}$	100	/	/	/
B		$5.1 \times 10^{-6}$	29	71	/	/

Afterwards, the structural characterization was performed by XRD on the main face of each sample after mechanical polishing. Mirror polished surfaces were obtained with the use of colloidal silica. XRD data were collected using a Bruker D8-Advance Diffractometer (LynxEye detector) in the reflexion geometry with  $\text{Cu-K}\alpha_{1,2}$  radiation ( $\lambda = 1.5418 \text{ \AA}$ ). The analyses were carried out at room temperature in an angular range of  $10^\circ < 2\theta < 100^\circ$ , with a step of 0.0257 and a total counting time of about 2h. XRD pattern of the three samples is presented in figure 2.

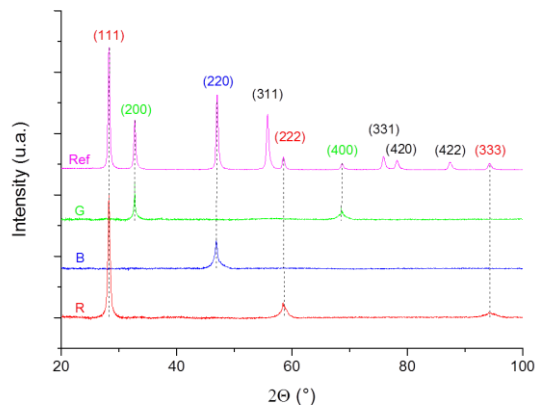


Figure 2. XRD pattern of the three  $\text{UO}_2$  single crystals for their major oriented surface after polishing, (100) surface for G sample, (110) surface for B sample and (111) surface for R sample. XRD pattern of  $\text{UO}_2$  powder as reference.

The XRD diagrams shows that each sample presents only XRD peaks of  $\text{UO}_2$ , excluding the presence of any additional phase. Unit cell parameter was evaluated to  $5.469 \pm 0.004 \text{ \AA}$ , which is in good agreement with that reported by Leinders *et al.*<sup>5</sup> for  $\text{UO}_2$  (i.e.  $a = 5.47127 \pm 0.00008 \text{ \AA}$ ). Moreover each surface is well oriented according to each pattern which showed only peaks corresponding to the main face orientation. Finally, the wide form of the peaks was due to the fact that XRD analysis was realised on bulk samples and not on powders, which is known as the flat plate phenomenon.

## Methods

### Dissolution tests

Dissolution tests were performed at room temperature under dynamic conditions and mechanical stirring, using 25 mL PTFE reactors continuously fed with nitric acid at room temperature. To limit waste production and to minimise the ratio between the mass of solid and the volume of the solution, nitric acid was recycled upstream the dissolution reactor and the total volume of solution in the closed circuit reached about 250 mL. The volumetric flow rate was  $30 \text{ mL.h}^{-1}$  in order to reduce perturbations at the solid / solution interface. Single crystals were put in  $2 \text{ mol.L}^{-1} \text{ HNO}_3$  for one month. At regular times, liquid samples of 5 mL were taken from the dissolution solution and replaced by the same volume of fresh nitric acid to maintain a constant volume of solution. After dilution of the liquid samples with  $0.2 \text{ mol.L}^{-1} \text{ HNO}_3$ , the total uranium concentration was analysed using inductively-coupled plasma mass spectrometry (ICP-MS, Thermo Fisher). The intensity of the signal was recorded at the mass of 238. ICP-MS analyses were calibrated using several uranium standard solutions prepared by dilution of a certified standard solution of 1000 ppm in uranium. The uranium concentrations in the solution were determined by using  $^{193}\text{Ir}$  as an internal standard and with three replicates. In these conditions, the detector limit for uranium reached  $0.1 \text{ ppb}$  (i.e.  $4.2 \times 10^{-10} \text{ mol.L}^{-1}$ ).

## Definitions and normalisation

Thanks to ICP-MS analyses, the elementary concentration,  $C(t)$  ( $\text{g}\cdot\text{L}^{-1}$ ), was determined for each given time  $t$ . The mass fraction of  $\text{UO}_2$  dissolved at time  $t$ ,  $\Delta m(t)$  (in %) was then calculated according to equation (4) :

$$\Delta m(t) = \frac{m(t)}{f_u \times m(t=0)} \times 100 = \frac{C(t) \times V}{f_u \times m(t=0)} \times 100 \quad (4)$$

where  $m(t)$  (expressed in g) corresponds to the total amount of the uranium released in solution at the given time  $t$  determined from  $C(t)$  and the volume of solution in contact with the solid,  $V$  (L);  $f_u$  (expressed in  $\text{g}\cdot\text{g}^{-1}$ ) is the mass ratio of the uranium in the solid and  $m(t=0)$  is the initial mass of the single crystal (g). The normalised weight loss for each sample,  $N_L(\text{U})$  ( $\text{g}\cdot\text{m}^{-2}$ ), was calculated according to equation (5) :

$$N_L(\text{U},t) = \frac{m(t)}{f_i \times S_T} \quad (5)$$

where  $S_T$  ( $\text{m}^2$ ) is the surface area of the solid in contact with the solution. As several oriented surfaces composed each sample, it was possible to determine the normalised weight loss for each oriented surface of one sample  $N_L^{(\text{hkl})}(\text{U})$  ( $\text{g}\cdot\text{m}^{-2}$ ), considering the following equation:

$$N_L(\text{U},t) = \sum \left( \frac{S_{(\text{hkl})}}{S_T} \times N_L^{(\text{hkl})}(\text{U},t) \right) = \sum \left( \frac{S_{(\text{hkl})}}{S_T} \times \frac{m_{(\text{hkl})}(t)}{f_u \times S_{(\text{hkl})}} \right) \quad (6)$$

where  $S_{(\text{hkl})}$  is the surface area of the oriented surface (hkl).

Dissolution rate can be also described using the dissolved thickness  $\text{Th}(t)$  ( $\mu\text{m}$ ) as a function of the time  $t$ , according to equation (7):

$$\text{Th}(t) = \frac{N_L(\text{U},t)}{\rho} \quad (7)$$

where  $\rho$  is the density of the solid ( $\text{g}\cdot\text{cm}^{-3}$ ), which is  $10.96 \text{ g}\cdot\text{cm}^{-3}$  for  $\text{UO}_2$ .

The normalised dissolution rates of each oriented surface,  $R_L^{(\text{hkl})}(\text{U},t)$  (expressed in  $\text{g}\cdot\text{m}^{-2}\cdot\text{d}^{-1}$ ) were derived from the normalised weight losses by time-derivation, i.e. :

$$R_L^{(\text{hkl})}(\text{U}) = \frac{dN_L^{(\text{hkl})}(\text{U},t)}{dt} \quad (8)$$

## RESULTS AND DISCUSSION

In order to determine the dissolution rate of  $\text{UO}_2$  single crystals and then to highlight the impact of the crystallographic orientation on the evolution of the normalised weight loss  $N_L^{(\text{hkl})}(\text{U})$  ( $\text{g}\cdot\text{m}^{-2}$ ), dissolution tests were performed on the three oriented  $\text{UO}_2$  single crystals. The evolution of the elemental uranium concentration, of

the dissolved mass and of dissolved thickness of the material during the dissolution of the three oriented  $\text{UO}_2$  single crystals is reported in figure 3.

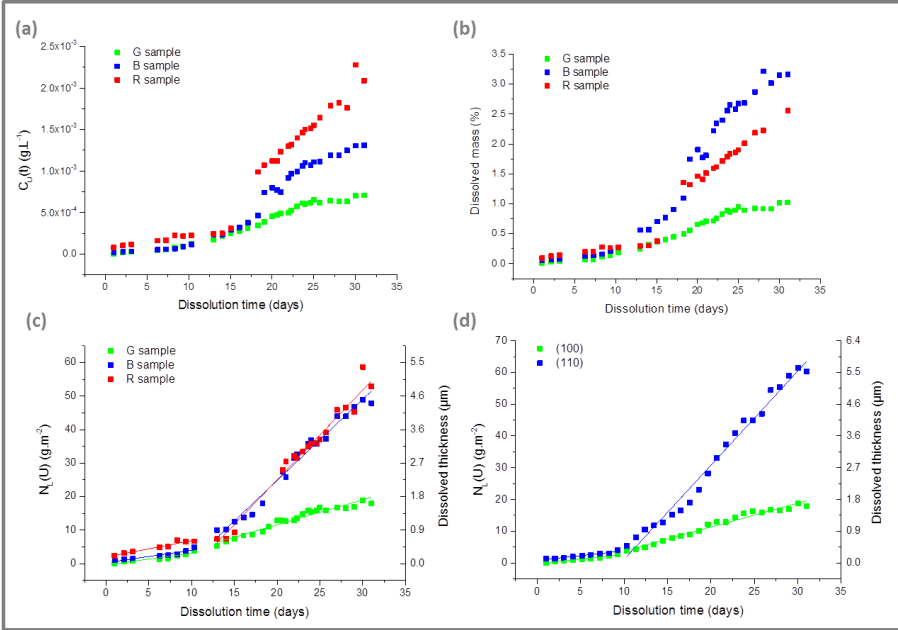


Figure 3. Evolution of uranium elementary concentration (a), of the dissolved mass (b), of the dissolved thickness and the normalised weight loss for entire samples (c) and of the dissolved thickness and the normalised weight loss for (hkl) oriented surfaces (d).

For all the samples, the uranium release is almost the same until 11 days of dissolution then became different, depending on the oriented sample, for longer dissolution times. The first stage occurs for  $\Delta m(t)/m_0 \leq 0.5$  wt.% and corresponded to the establishment of a steady state. This period is called “induction time” in the literature <sup>6</sup>. During this step, the normalized weight losses  $N_L(U)$  and the associated dissolved masses increases linearly with time, which allows the accurate determination of the normalized dissolution rates  $R_{L,0}(\text{g.m}^{-1}.\text{d}^{-1})$ . This phenomenon is observed for all samples investigated, which showed that the crystal orientation of the surface did not play any important role on this first step of dissolution. The normalised dissolution rates determined during this first step for the three samples are reported in Table 2.

After about 11 days of dissolution (i.e. for  $\Delta m(t)/m_0 > 0.5$  wt.%), a second dissolution step is observed. Uranium is released faster in solution with some differences depending on the nature of the  $\text{UO}_2$  single crystal (Table 2). Two hypotheses could explain this increase. First, the reactive surface area may increase at the solid/liquid interface due to the progress of the dissolution reaction (appearance of roughness, pores, corrosion pits ...). Secondly, the dissolution reaction (1) may lead to the production of catalytic species in quantities high enough to induce the development of the autocatalytic reaction, already mentioned for powdered and sintered samples of  $\text{UO}_2$  dissolution in nitric acid media.

Table 2. Normalised dissolution rates  $R_L(U)$  ( $\text{g}\cdot\text{m}^{-2}\cdot\text{d}^{-1}$ ) determined during the two steps of dissolution for each sample and normalised dissolution rates  $R_L^{(hkl)}(U)$  ( $\text{g}\cdot\text{m}^{-2}\cdot\text{d}^{-1}$ ) for each (hkl) orientation surface.

$R_L(U)$ ( $\text{g}\cdot\text{m}^{-2}\cdot\text{d}^{-1}$ )	R sample	G sample	B sample
First step	$0.49 \pm 0.10$	$0.34 \pm 0.08$	$0.37 \pm 0.10$
Second step	$2.67 \pm 0.16$	$0.74 \pm 0.08$	$2.42 \pm 0.16$
$R_L^{(hkl)}(U)$ ( $\text{g}\cdot\text{m}^{-2}\cdot\text{d}^{-1}$ )	(111)	(100)	(110)
First step	/	$0.28 \pm 0.05$	$0.30 \pm 0.06$
Second step	/	$0.75 \pm 0.06$	$2.97 \pm 0.18$

The normalised weight losses obtained during the second step of the dissolution for the single crystals called R and B is found to be more important than that obtained for single crystal G. This difference is correlated to the percentage of each oriented surfaces in the different samples. Indeed, while the orientation of the surface has no significant impact on the normalized dissolution rates during the first step, it is found to affect the normalized dissolution rate during the second step.

In order to evaluate such a difference, the normalised weight losses of the oriented surfaces (100) and (110),  $N_L^{(hkl)}(U)$  ( $\text{g}\cdot\text{m}^{-2}$ ) were evaluated considering Eq. (3), leading to the determination of  $R_L^{(100)}(U)$  and  $R_L^{(110)}(U)$ . Values are reported in Table 2. The (100) surface dissolves slower than (110) orientation. One potential explanation can be the nature of the successive planes present at the surface. Indeed, from the crystallographic representation of each oriented surfaces (fig. 1), the atomic planes of (110) oriented surface are composed of both uranium and oxygen atoms. Godinho *et al*<sup>7</sup> already showed during the dissolution of  $\text{CaF}_2$  (fluorite) that such planes (containing either Ca and F) were preferentially dissolved, which could be explained by the polarity character of this surface<sup>8</sup>. On the contrary, the (100) surface is made of an alternation of planes containing uranium atoms only or oxygen atoms only. This surface containing terminal oxygen atoms leads to a non-polarise surface, preventing uranium oxidation. Eventually, the  $N_L^{(111)}(U)$  cannot be calculated yet, because of a lack of data concerning the  $(1\bar{2}1)$  surface dissolution.

## CONCLUSION

Dissolution study of oriented  $\text{UO}_2$  single crystals in nitric acid medium and at room temperature showed two successive steps for of the three oriented single crystals studied/investigated. The first step occurred for a weight loss under 0.5%. This step corresponds to the establishment of a steady state during which the dissolution rate is not controlled by the surface orientation and could be considered as a constant. The dissolution rate of this first step, called “induction period” in the literature, is about  $0.34\text{--}0.49 \text{ g}\cdot\text{m}^{-2}\cdot\text{d}^{-1}$ .

The second step is characterized by a strong increase of the normalised dissolution rate with dissolution time leading to a second linear evolution of the normalised weight loss  $N_L(U)$ . This increase could be explained by an increase in the reactive surface area at the solid/liquid interface due to the progress of the dissolution reaction (appearance of roughness, pores, corrosion pits ...) or by the formation of catalytic species in quantities high enough to induce the development of the autocatalytic reaction. During this state, the orientation of the surface had significant impact on the

normalized dissolution rates. Then the individual normalised weight losses of the oriented surfaces (100) and (110),  $N_L^{(hkl)}(\text{U})$  ( $\text{g}\cdot\text{m}^{-2}$ ) were evaluated and revealed that the (100) surface dissolved slower than (110) orientation. Surfaces which are composed of both uranium and oxygen atoms, such as the (110) face, were preferentially dissolved, which could be explained by the polarity character of this surface.

## References

- (1) Herrmann, B. Dissolution de pastilles d' $\text{UO}_2$  non irradiées dans l'acide nitrique. *Projet de retraitement et de traitement des déchets* **1984**, Ref. KfK 3673.
- (2) Nishimura, K. Chikazawa, T. Hasegawa, S. Tanaka, H. Ikeda, Y. Yasuike, Y. Takashima, Y. Effect of nitrous acid on dissolution of  $\text{UO}_2$  powders in nitric acid optimal conditions for dissolving  $\text{UO}_2$ . *Journal of Nuclear Science and Technology* **1995**, 32 (2), 157–159
- (3) Fukasawa, T. Relationship between dissolution rate of uranium-dioxide pellets in nitric-acid solutions and their porosity. *Journal of Radioanalytical and Nuclear* **1986**, 106, 345–356.
- (4) Taylor, R. F. Sharratt, E. W. Chazal, L. E. M. Logsdail, D. H. Dissolution rates of uranium dioxide sintered pellets in nitric acid systems. *Journal of Applied Chemistry* **1963**, 13, 32–40.
- (5) Leinders, G. Cardinaels, T. Binnemans, K. Verwerf, M. Accurate lattice parameter measurements of stoichiometric uranium dioxide. *Journal of Nuclear Materials* **2015**,
- (6) Cordara, T. Szenknect, S. Claparede, L. Podor, R. Mesbah, A. Lavalette, C. Dacheux, N. Kinetics of dissolution of  $\text{UO}_2$  in nitric acid solutions: a multiparametric study of the non-catalysed reaction. *Journal of Nuclear Materials* **2017**, 496, 251–264.
- (7) Godinho, J. R. A. Piazzolo, S. Evins, L. Z. Effect of surface orientation on dissolution rates and topography of  $\text{CaF}_2$ . *Geochimica et Cosmochimica Acta* **2012**, 86, 392–403.
- (8) Rennie, S. Bright, E. L. Sutcliffe, J. E. Darnbrough, J. E. Rawle, J. Nicklin, C. Lander, G. H. Springell, R. The role of crystal orientation in the dissolution of  $\text{UO}_2$  thin films. *Corrosion science* **2018**, 145, 162–169.